IEEE Access
Multidisciplinary ⋮ Rapid Review ⋮ Open Access Journal

Received 25 June 2024, accepted 12 July 2024, date of publication 17 July 2024, date of current version 26 July 2024.

Digital Object Identifier 10.1109/ACCESS.2024.3429199

RESEARCH ARTICLE

Research on Passenger Flow Congestion Propagation of Multi-Level Rail Transit Considering Stopping Scheme

CHANGFENG ZHU, JINXIU JIA, JINHAO FANG, JIE WANG, LINNA CHENG, RUNTIAN HE, AND CHAO ZHANG

School of Traffic and Transportation, Lanzhou Jiaotong University, Lanzhou 730070, China

Corresponding author: Jinxiu Jia (jxjia12@163.com)

This work was supported in part by the National Natural Science Foundation of China under Grant 72161024, and in part by the "Double-First Class" Major Research Programs, Educational Department of Gansu Province under Grant GSSYLXM-04.

ABSTRACT Due to the complex operational characteristics of multi-level rail transit networks, such as cross-system and multi-level, passenger flow congestion must not only consider the steady state of homogeneous transportation networks but also reveal the deep-seated mechanism of congestion spreading between heterogeneous transportation networks. An analysis theory of travel paths based on Improved Prospect Theory (IPT) is proposed using generalized travel time and congestion degree as dual reference points. By organically integrating passenger travel modes and routes, a two-layer model of passenger travel mode selection based on Nested Logit-Improved Prospect Theory (NL-IPT) is constructed. On this basis, considering key influencing factors such as the stopping scheme, an improved Susceptible-Infected-Recovered (SIR) model of multi-level rail transit passenger flow congestion propagation under bounded rationality conditions is proposed. Taking the multi-level rail transit in Beijing, China, as an example, the propagation process of passenger flow congestion in multi-level rail transit is simulated and analyzed. Through the sensitivity analysis of critical factors such as gain and loss sensitivity coefficient, propagation rate, and recovery rate, the mechanism of the influence of key parameters on passenger flow congestion propagation is revealed. The results show that when the proportion of waiting passengers heading to subsequent stops of the arriving train is greater than or equal to 0.6, there will be slight fluctuations in the initial stage of congestion propagation. When this proportion decreases by 80%, the congestion propagation range decreases by 23.3%. The research provides a reference for the operation plans and management optimization of multi-level rail transit.

INDEX TERMS Multi-level rail transit, passenger flow congestion propagation, stopping scheme, improved prospect theory, improved SIR model.

I. INTRODUCTION

The spatiotemporal constraints and basic laws of passenger travel activities are the key to the collaborative optimization of metropolitan area space and transportation networks. With the development and evolution of urban agglomerations and metropolitan areas, a multi-level rail transit network with interconnection and integrated operation has gradually formed. While significantly improving transportation accessibility and passenger travel convenience and efficiency, it also puts higher requirements for multi-level rail transit network operation organizations. In particular, frequent passenger flow congestion during peak periods and heavy passenger flow periods poses specific challenges to the operational efficiency and safety of multi-level rail transit systems. Due to the complex operational characteristics such as cross-system and multi-level organization, passenger flow congestion in multi-level rail transit networks not

The associate editor coordinating the review of this manuscript and approving it for publication was Emanuele Crisostomi.

only disrupts the steady state of homogeneous networks but also easily leads to cross-level congestion propagation. This increases the probability, intensity, and influence range of passenger flow congestion, directly affecting transportation efficiency and safety risks. Therefore, analyzing the influencing factors of large passenger flow congestion propagation and revealing the complex mechanism of multi-level rail transit passenger flow congestion propagation is not only helpful to optimize the operation efficiency of multi-level rail transit system and improve passenger travel experience, but also the key to ensure the safe and stable operation of trains and realize the sustainable development of transportation.

The congestion propagation characteristics of traffic networks were first studied in 1998. Wright and Roberg [1] established a traffic congestion propagation model caused by a single bottleneck, which provided a direction for solving urban traffic congestion problems. Subsequently, domestic scholars began to pay attention to road traffic congestion propagation in 2004. Considering that the propagation process of urban traffic network congestion is similar to virus propagation, Wu et al. [2] innovatively introduced the Susceptible-Infective-Recovered (SIR) virus propagation model into analyzing urban traffic network congestion propagation mechanism. On this basis, Zheng et al. [3] conducted an in-depth study of the congestion degree and efficiency in complex transportation networks by introducing the congestion effect. Li et al. [4] studied the impact of network topology on traffic congestion through an improved traffic flow model. Saberi et al. [5] used the SIR model to dynamically describe the changing process of traffic congestion propagation in urban networks, providing an effective tool for predicting and controlling the proportion of congested road sections in the network. Priambodo et al. [6] combined the clustering method of grey level of co-occurrence matrix and spectral clustering and the hidden Markov model to predict the impact of road congestion on traffic status.

With the rapid development of rail transit, its passenger congestion propagation problem has gradually become prominent, which has attracted the attention of many scholars. Du et al. [7] used the SOM neural network and fuzzy classification algorithm to accurately classify multi-index data and implemented urban rail station classification for congestion propagation blocking. Chen et al. [8] combined multi-dimensional attribute characteristics such as passenger flow, platforms, and trains to establish a rail transit station capacity model that considers congestion propagation. From the perspective of research methods, the literature [9], [10], [11], [12] conducted an in-depth study of the congestion propagation mechanism of urban rail transit passenger flow based on the principle of cellular automata, providing an essential perspective for revealing the dynamic evolution process of passenger flow congestion. Sun et al. [13] and Huang et al. [14] proposed a weighted cascade failure model based on the coupled map lattice model (Coupled Map Lattice, CML). The vulnerabilities of Beijing's urban rail transit network and the multimodal transport network coupled with bus and urban rail were assessed, respectively. Zhang et al. [15] further expanded the application of the CML model. They proposed the ICML model to study the impact of different attack strategies on the vulnerability of urban rail transit networks. Xiong and Yao [16] integrated factors such as physical structure, network initial traffic status, and passenger flow into the CML model, quantified the model parameters through passenger flow data and constructed a rail transit congestion propagation model with more practical application value. Zhang et al. [17] used two malicious attack methods to conduct an in-depth study of the vulnerability of subway networks. They performed a comparative analysis of the characteristics and vulnerabilities of subway networks in different cities. Based on travel behavior analysis, Liu et al. [18] constructed a flow-weighted urban rail transit network cascading failure model to evaluate network vulnerability.

Compared with the above methods, the SIR virus propagation model has been widely used in studying urban rail passenger congestion propagation mechanisms because it can dynamically simulate the development process of congestion and exhibit high timeliness. Xiong and Yao [19] built a quantitative model of congestion propagation rate based on the epidemic model and deeply analyzed the impact of passenger flow on rail transit congestion propagation. To simulate the congestion propagation process more accurately, Zeng and Li [20] not only constructed a congestion propagation model based on the SIR model but also further introduced six influencing factors, such as the gray system model and passenger flow, to establish a comprehensive quantitative model of the propagation rate. Shi et al. [21] used the classic SIR model to study passenger flow's congestion propagation rules systematically and analyzed the model's sensitivity to each parameter. In addition, Wang et al. [22] innovatively combined random regret minimization theory, cellular automaton model, and ASEIR (advanced susceptible-exposed-infectious-recovered) model in their research to construct a model that considers passengers under emergencies. Urban rail passenger congestion propagation model of travel choice behavior.

The above research mainly delves into the congestion propagation process of road traffic and rail transit based on single-layer networks. With the increasing complexity and diversification of urban transportation systems, scholars have begun to pay attention to traffic congestion propagation in multi-layer networks. Ding et al. [23] explored the impact of different road network topologies and characteristics on traffic congestion propagation from the perspective of multi-layer urban transportation networks. Subsequently, Ma et al. [24] analyzed the intrinsic relationship between urban traffic carrying capacity and traffic congestion based on multiple networks. They proposed targeted control strategies to alleviate urban road congestion problems effectively. To more effectively ease traffic congestion on multi-level

TABLE 1. Comparative analysis of previously published research on the passenger flow congestion propagation.

Research scope	Publications	Research problem	Solution	Limitation
Single-layer network	Xiong and Yao [19]	Quantification of the passenger flow congestion propagation rate in urban rail transit	SIR model	Only the congestion propagation in urban rail transit networks is considered (without considering multi-mode rail transit); Neglecting the impact of traveler behavior on the propagation of passenger congestion.
	Zeng and Li [20]	Congestion propagation in oversaturated urban rail transit	SIR model; Gray system model	
	Shi et al. [21]	Urban rail traffic congestion propagation and control strategy	SIR model	
	Wang et al. [22]	Passenger flow congestion propagation in urban rail transit	random regret minimization theory; cellular automaton model; ASEIR model	Not involving the passenger flow congestion propagation of multi-level rail transit.
Multi-layer network	Zhu et al. [31]	Congestion propagation of double-layer urban rail transit	CML model	Neglecting the consideration of the stopping scheme.
	Jia et al. [32]	Multi-level rail transit passenger flow congestion propagation	SIR model	

networks, Zhang et al. [25] and Gao et al. [26] proposed multi-level network resource allocation strategies and traffic flow allocation strategies to enhance urban traffic carrying capacity effectively.

Many scholars have explored the factors influencing congestion propagation in recent years. Based on the multi-level complex network of urban roads, Zhou et al. [27] and Huang et al. [28] studied the coupled propagation dynamics between early warning information, traffic guidance information, and traffic congestion. At the same time, as a critical factor affecting urban traffic conditions, traveler behavior has also attracted wide attention from scholars. Guo and Xu [29] discussed the problem of multiple network risk propagation under herd mentality and risk preference. Huang and Sun [30] further studied the influence of traveler behavior on traffic congestion propagation. They constructed a multi-coupling network congestion risk propagation model of urban road networks, early warning information propagation networks, and resident travel networks.

The above research mainly focuses on congestion propagation in multi-layer road traffic networks, while the discussion on passenger flow congestion in multi-layer rail transit networks is relatively insufficient. To this end, the team is actively engaged in this research field and strives to explore and contribute to this area more in-depth. Based on fully considering the bounded rationality of passengers, Zhu et al. [31] innovatively constructed a congestion propagation model of a two-layer urban rail transit network based on the CML model. Jia et al. [32] constructed a multi-level rail transit passenger flow congestion propagation model based on the SIR infectious disease model and quantitatively analyzed the critical parameters in the model. However, the existing research has not fully considered the influence of passenger travel choice behavior and train stopping scheme when constructing the model. The passenger's travel choice behavior and the train stopping scheme directly affect passenger flow distribution, significantly impacting the congestion propagation process. Therefore, to more accurately reveal the propagation mechanism of rail transit passenger flow congestion, it is necessary to consider the above vital factors fully.

Many scholars have researched the train stopping scheme under large passenger flow. Aiming at the problem of large passenger flow agglomeration in urban rail transit, Zhou et al. [33] constructed a reasonable stop adjustment optimization model for trains with sudden large passenger flow on the line. Meng et al. [34] proposed a collaborative optimization model of urban rail train diagram and station current limits considering the skip-stop strategy for the subway system's increasingly severe congestion and passenger flow oversaturation. Hu et al. [35] proposed an integrated train operation adjustment method from the perspective of late recovery and passenger retention mitigation, including a time-exceeding strategy, a train deduction strategy, a skip-stop strategy, and implementing dynamic stop time. Tao et al. [36] studied the optimization of the stop-skipping strategy of the subway in view of the extreme congestion of the passenger flow on the oversaturated subway line during the peak period. They balanced the passenger flow distribution and train service capacity by optimizing the stop-skipping strategy. Zhang et al. [37] optimized the train stopping scheme for the problem of passenger detention caused by train capacity constraints during peak hours, aiming to improve the train transportation capacity by adjusting the stopping scheme.

The comparative analysis of research results related to passenger congestion propagation is shown in Table 1.

Based on this, this paper takes the multi-level rail transit network as the research object. It sets generalized travel time and congestion degree as ''double reference points'' based on fully considering the ''bounded rationality'' factors in passengers' travel decision-making. The prospect value of Improved Prospect Theory (IPT) is introduced as the utility value in the Nested Logit (NL) model, and a passenger travel behavior selection model based on the Nested Logit-Improved

Prospect Theory (NL-IPT) model is constructed. On this basis, considering the critical factor of the train stopping scheme, an improved SIR model is proposed. Taking the line time-divided section passenger flow, line section full load rate, station inbound and outbound passenger flow, transfer passenger flow at transfer stations, train timetable, and vehicle marshaling as input conditions, and the congestion propagation range as output, a multi-level rail transit passenger flow congestion propagation model is constructed. The intrinsic mechanism of passenger flow congestion propagation in multi-level rail transit networks is revealed through case simulation analysis.

II. ANALYSIS OF PASSENGER TRAVEL CHOICE BEHAVIOR BASED ON IPT

A. TRAVEL PATH PERCEPTION UTILITY BASED ON IPT

Set $A = \{d \,|d = 1, 2, \cdots, D\}$ as a multi-level rail transit subnetwork. The station h is located in subnetwork o, the station m is situated in subnetwork d, and $o \neq d$. The set of travel paths between h and m is $C = \{k|\, k = 1, 2, \cdots, K\}$. Cost and walking distance conversion weights [38] are introduced to convert costs and walking distance into time. Generalized travel time and congestion level are ''dual reference points''. Then, the generalized travel time of the travel path k between h-m is

$$u_{hm}^{k} = u_{hm}^{k,\text{time}} + \xi \cdot (480 \times q \times z^{k}/x) + \upsilon \cdot s^{k}/i \tag{1}$$

where $u_{hm}^{k,\text{time}}$ is the actual travel time of the path k between $h$and m. q is the legal working days. z^{k} is the travel cost of path k. x is per capita annual income. s^{k} is the walking distance of path k. i is the average speed of passengers walking. ξ and υ respectively represent the conversion weights of cost and walking distance, reflecting the sensitivity differences of passengers to travel time, cost, and walking distance.

According to the tolerance of travel time, the travel types are divided into flexible and rigid travel [39]. The late penalty cost describes the preference change phenomenon in rigid travel. The time value function under the improved flexible travel and rigid travel scenarios are as follows:

$$v_{\text{flexible}}(u_{hm}^{k}) = \begin{cases} (u_{hm}^{0} - u_{hm}^{k})^{\alpha} & u_{hm}^{k} \leq u_{hm}^{0} \\ -\chi(u_{hm}^{k} - u_{hm}^{0})^{\beta} & u_{hm}^{k} > u_{hm}^{0} \end{cases} \tag{2}$$

$$v_{\text{rigid}}(u_{hm}^{k}) = \begin{cases} (u_{hm}^{0} - u_{hm}^{k})^{\alpha} & u_{hm}^{k} \leq u_{hm}^{0} \\ -\chi(u_{hm}^{k} - u_{hm}^{0})^{\beta} - b & u_{hm}^{k} > u_{hm}^{0} \end{cases} \tag{3}$$

$$u_{hm}^{0} = \frac{\sum_{k=1}^{K} u_{hm}^{k}}{K} \tag{4}$$

where u_{hm}^{0} is the generalized travel time reference point between h and m, which is determined by the average value of the generalized travel time of each path. α is the gain sensitivity coefficient, $0 < \alpha \leq 1$. β is the loss sensitivity coefficient, $0 < \beta \leq 1$. χ is the loss aversion coefficient, $\chi \geq 1$. b is the late penalty cost that may exist in rigid travel activities such as commuting and business meetings, $b \geq 0$. According to the calibration of existing research [40], $\alpha = \beta = 0.88$, $\chi = 2.25$.

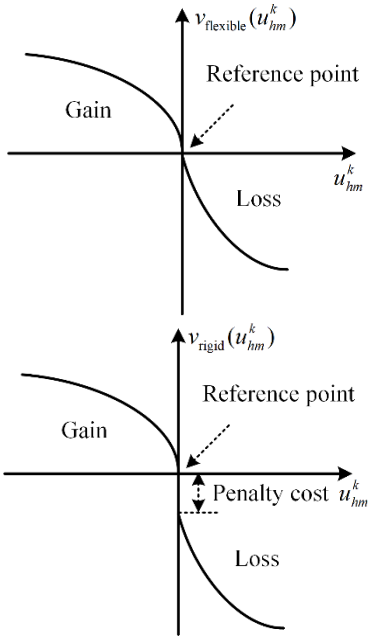

FIGURE 1. Improved generalized travel time value function curve. (a) Flexible travel. (b) Rigid travel.

Fig. 1 shows the improved time value function images under flexible and rigid travel scenarios.

As shown in Fig. 1, when $u_{hm}^{k} \leq u_{hm}^{0}$, the actual travel time is less than the reference point, and the traveler's psychological perception is a gain; when $u_{hm}^{k} > u_{hm}^{0}$, the actual travel time is greater than the reference point, and the traveler's psychological perception is a loss. Additionally, the introduction of the penalty cost b significantly reduces the overall utility of a certain travel mode when lateness occurs.

The section full load rate index is used to evaluate the degree of congestion, and the value function of the degree of congestion is

$$v(c_{hm}^{k}) = \begin{cases} (c_{hm}^{0} - c_{hm}^{k})^{\alpha} & c_{hm}^{k} \leq c_{hm}^{0} \\ -\chi(c_{hm}^{k} - c_{hm}^{0})^{\beta} & c_{hm}^{0} < c_{hm}^{k} \end{cases} \tag{5}$$

$$c_{hm}^{0} = \frac{\sum_{k=1}^{K} c_{hm}^{k}}{K} \tag{6}$$

where c_{hm}^{k} is the congestion degree of the travel path k between h and m. c_{hm}^{0} is the congestion degree reference point between h and m, which is determined by the average congestion degree of each path.

According to literature [39], equation (4) shows the improved decision weight function and Fig. 2 shows the original and improved function curves.

$$\omega(l_{hm}^{k}) = \frac{\delta(l_{hm}^{k})^{\rho}}{(1 - l_{hm}^{k})^{\rho} + \delta(l_{hm}^{k})^{\rho}}, \rho > 1 \tag{7}$$

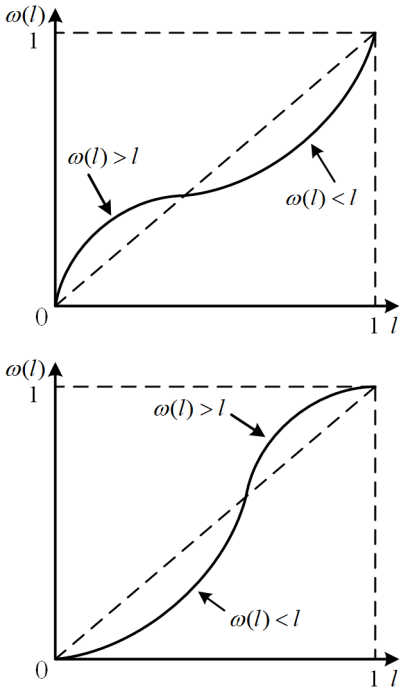

FIGURE 2. Decision weight function curve. (a) The original decision weight function. (b) Improved decision weight function.

where l_{hm}^{k} is the actual probability of selecting the travel path k. δ is the discrimination parameter. ρ is the attraction parameter.

As shown in Fig. 2, when making travel decisions, people rarely pay attention to unexpected situations with a small probability of occurrence and therefore underestimate small probabilities. That is, when $l \to 0$, $\omega(l) < l$. However, when estimating travel times, individuals subjectively expect to arrive at the expected time and assign a higher subjective probability to this expected travel time than the objective probability. That is, when $l \to 1$, $\omega(l) > l$.

Based on this, the generalized travel time and congestion degree prospect value of the travel path k between h and m are

$$V_{hm}^{k}(u) = v(u_{hm}^{k})\omega(l_{hm}^{k}) \tag{8}$$

$$V_{hm}^{k}(c) = v(c_{hm}^{k})\omega(l_{hm}^{k}) \tag{9}$$

When calculating the comprehensive perceived value of the path, it must be made dimensionless.

$$\bar{V}_{hm}^{k} = \frac{V_{hm}^{k}}{\max\{|V_{hm}|\}} \tag{10}$$

Assume ϑ_{u}^{k} and ϑ_{c}^{k} are the decision preference coefficients of generalized travel time and congestion degree, respectively, and $\vartheta_{u}^{k} + \vartheta_{c}^{k} = 1$, then, the perceived utility of the travel path k between h and m is

$$U_{hm}^{k} = \vartheta_{u}^{k}\bar{V}_{hm}^{k}(u) + \vartheta_{c}^{k}\bar{V}_{hm}^{k}(c) \tag{11}$$

B. PASSENGER TRAVEL CHOICE MODEL BASED ON NL-IPT

A two-layer NL model is constructed using the travel mode as the upper choice limb and the specific paths under the travel mode as the lower choice limb. Assuming that the alternative path set C is divided into Y travel modes, then the travel mode set $Z = \{y|\, y = 1, 2, \cdots, Y\}$, and $A \subseteq Z$. Define K_y as the number of travel paths in travel mode y, that is, $K = K_1 + K_2 + \cdots + K_Y$. The probability $p_{hm}(k\,|y)$ of choosing path k in travel mode y is

$$p_{hm}(k\,|y) = \frac{\exp\left(\eta \cdot U_{hm}^{ky}/\theta_y \cdot \max\left\{\left|U_{hm}^{ky}\right|\right\}\right)}{\sum_{k=1}^{K_y}\exp\left(\eta \cdot U_{hm}^{ky}/\theta_y \cdot \max\left\{\left|U_{hm}^{ky}\right|\right\}\right)} \tag{12}$$

where η is the familiarity index of passengers with the travel path. θ_y is a dissimilar parameter of travel mode y, reflecting the degree of correlation between the various paths in travel mode y. $0 \le \theta_y \le 1$, the larger the value, the smaller the correlation. When $\theta_y = 1$, the paths are independent of each other. U_{hm}^{ky} represents the transaction utility of path k in travel mode y.

The utility H_{hm}^{y} and probability $p_{hm}(y)$ of choosing travel mode y between h and m are:

$$H_{hm}^{y} = \sum_{k=1}^{K_y} p_{hm}(k\,|y) \cdot U_{hm}^{ky} / \max\left\{\left|U_{hm}^{ky}\right|\right\} \tag{13}$$

$$p_{hm}(y) = \frac{\exp\left(\phi \cdot H_{hm}^{y} + \theta_y \cdot \Gamma_y\right)}{\sum_{y=1}^{Y}\exp\left(\phi \cdot H_{hm}^{y} + \theta_y \cdot \Gamma_y\right)} \tag{14}$$

where ϕ is the passenger's familiarity with the travel mode. θ_y is the correlation between the various paths in the travel mode y, and the value range is [0, 1]. Γ_y is the logsum value, which can be expressed as

$$\Gamma = \ln\left[\sum_{k=1}^{K_y}\exp\left(\eta \cdot U_{hm}^{ky}/\theta_y \cdot \max\left\{\left|U_{hm}^{ky}\right|\right\}\right)\right] \tag{15}$$

In summary, Fig. 3 shows the process of portraying passenger travel choice behavior using the NL-PT model.

III. CONSTRUCTION OF CONGESTION PROPAGATION MODEL

A. ANALYSIS OF CONGESTION PROPAGATION RATE CONSIDERING STOPPING SCHEME

According to the passenger flow demand on the line, the stopping scheme of the train is reasonably determined. By coordinating the waiting time of the passengers at the station and the waiting time of the passengers on the train, the purpose of reducing the total travel time of the passengers can be achieved. In addition, the cross-station mode can also adjust the congestion degree of passengers in the train through the train stop sequence.

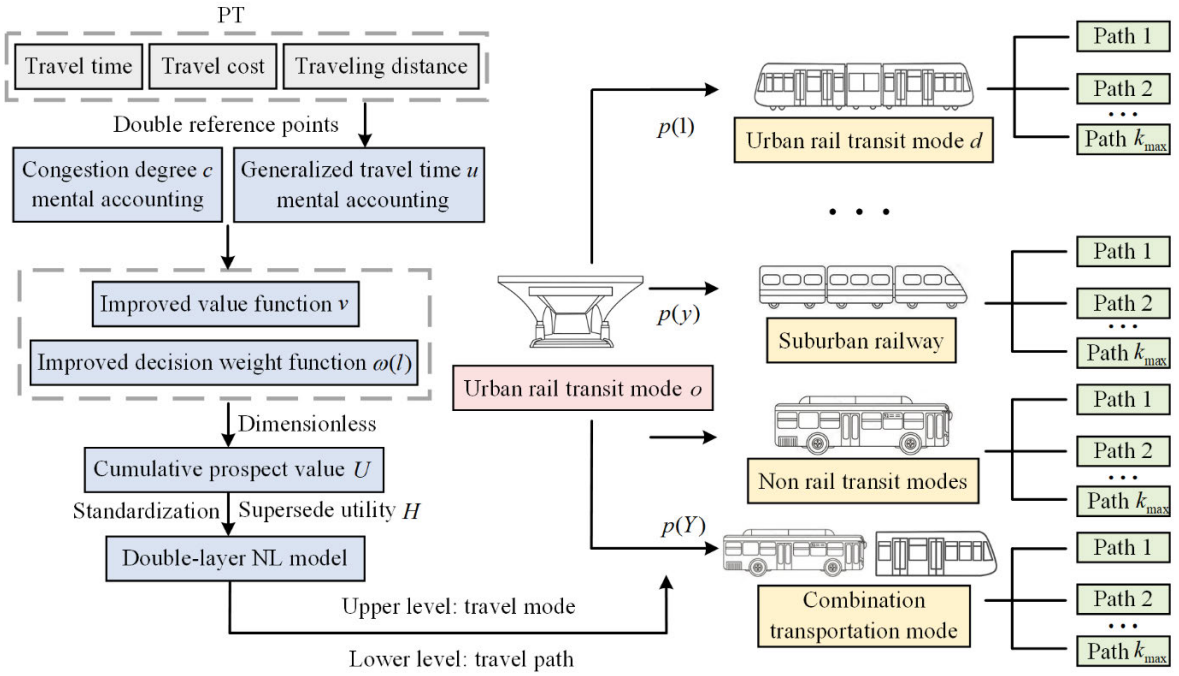

FIGURE 3. Flowchart of NL-PT model portraying passengers' travel choice behavior.

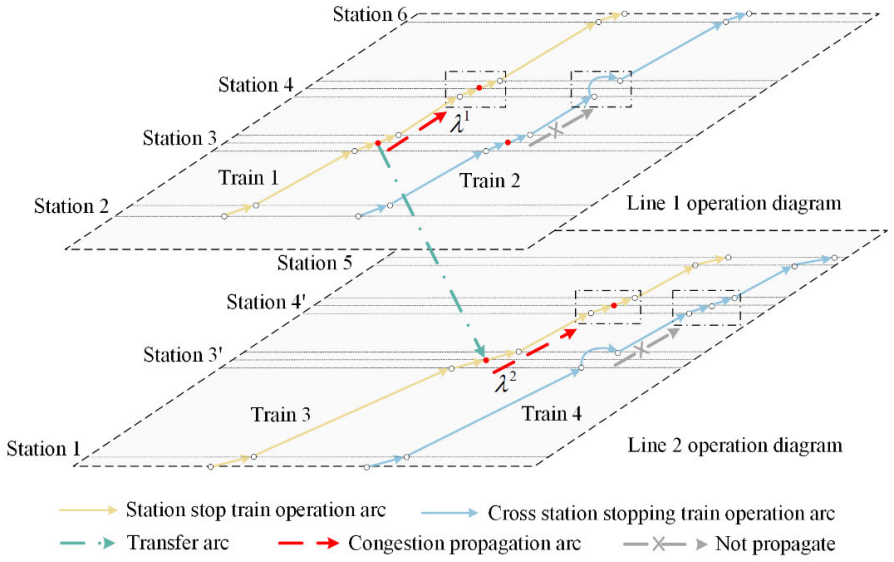

FIGURE 4. The influence of the stopping scheme on the congestion propagation process.

Different train stopping schemes have significant differences in the propagation effect of passenger congestion, which directly affects the flow pattern of passengers between the platform and the train, changes the distribution of the number of passengers on the platform and the train, and then affects the propagation rate and recovery rate of congestion in the system. Fig. 4 shows the influence of different stopping schemes on congestion propagation.

Fig. 4 shows that Train 1 stops at the congested Station 3 and its subsequent Station 4, so the congestion may spread to Station 4 through these stops. Since Train 2 does not stop at Station 4, its congestion at Station 3 will not affect Station 4. Additionally, when passengers of Line 1 transfer to Line 2 at Station 3, congestion may spread to Line 2, increasing its passenger flow pressure. Therefore, optimizing the design and management of transfer stations is crucial for reducing the spread of cross-line congestion. Finally, Train 4 does not

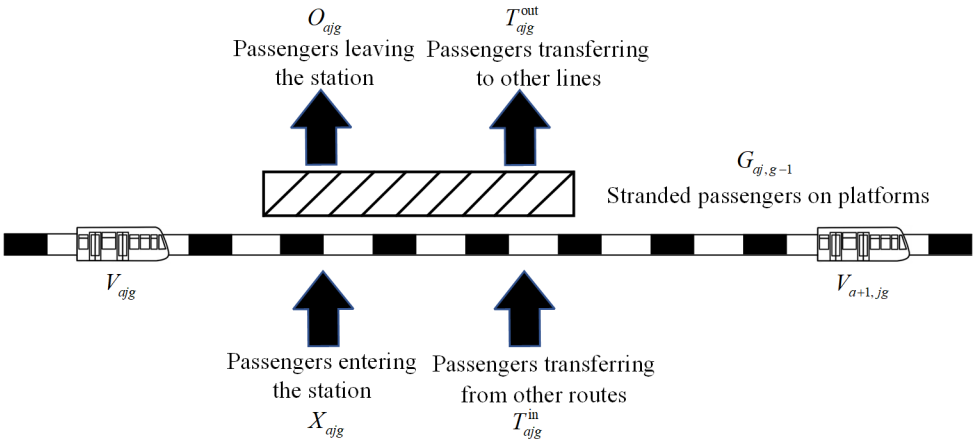

FIGURE 5. The flow state of platform and train passengers.

stop at Station 3, so it will not spread the congestion from Station 3 to Station 4.

The propagation speed of congestion caused by large passenger flow largely depends on the section's full load rate and transfer rate, which are determined by the dynamic changes of passenger flow on the platform and train after the train arrives at the station. Fig. 5 shows the distribution of platform and train passengers.

1) NUMBER OF PASSENGERS ON THE PLATFORM

Fig. 5 depicts that the change in the number of passengers on the platform during the interval between the departure of the train and the previous train is determined by the number of passengers stranded on the platform, passengers entering the station, and passengers transferring. Station a has attribute γ_a, which takes 1 when trains can cross the station and 0 when trains cannot cross the station. Train g has attribute ε_g^a, which takes 1 when the train passes through station a without stopping and 0 when it stops at station a.

Passengers decide whether to take train g based on whether train g stops at their target station. Therefore, the number of passengers waiting for the platform when the train g reaches the station a of line j is as follows:

$$P_{ajg} = G_{aj,g-1} + X_{ajg} + T^{in}_{ajg} \tag{16}$$

where G_{ajg} is the number of passengers stranded on the platform when train g leaves station a of line j. X_{ajg} is the number of passengers entering station a of line j within the departure interval between train $g-1$ and train g. T^{in}_{ajg} is the number of passengers transferred from other lines to station a of line j within the departure interval between train $g-1$ and train g.

When train g arrives at station a of line j, the number of passengers waiting for train g at the platform is:

$$F_{ajg} = \begin{cases} 0 & \varepsilon_g^a = 1, \gamma_a = 1 \\ P_{ajg} & \varepsilon_g^a = 0 \\ P_{ajg} \cdot \varphi_{ajg} & \varepsilon_g^a = 1, \gamma_a = 0 \end{cases} \tag{17}$$

where φ_{ajg} is the proportion of passengers waiting on the platform who plan to go to the subsequent stop of train g when train g using the cross-stop mode stops at station a on line j.

2) NUMBER OF TRAIN PASSENGERS

Fig. 5 depicts that after the train stops, the actual number of passengers getting on the train is determined by the boarding demand of passengers on the platform and the remaining capacity of the train. Then, the number of passengers carried by train g before arriving at station $a+1$ on line j is

$$V_{a+1,jg} = V_{ajg} - O_{ajg} - T^{\text{out}}_{ajg} + B_{ajg} \tag{18}$$

Of which:

$$B_{ajg} = \min\left\{M_{ajg} + O_{ajg} + T^{\text{out}}_{ajg}, F_{ajg}\right\} \tag{19}$$

where O_{ajg} is the number of passengers leaving the station when the train g reaches the station a of line j. T^{out}_{ajg} is the number of passengers transferred by train g from station a of line j to other lines. B_{ajg} is the number of passengers who successfully get on the train when the train g stops at station a of line j. M_{ajg} is the residual passenger capacity of train g before it reaches station a of line j.

In summary, the congestion propagation rate of station a on line j at time t is

$$\lambda_{taj} = 1 - \exp\left\{-\left[\frac{V_{a+1,jg}}{Q_{\max}} + \frac{T^{\text{in}}_{ajg}}{\sum_j \left(T^{\text{in}}_{ajg} + T^{\text{out}}_{ajg}\right)} \cdot \tau_a\right]\right\} \tag{20}$$

where $Q_{\max}$ is the maximum passenger capacity of the train. τ_a is a 0-1 variable, which takes 1 if the congested station is a transfer station for a certain rail transit system; otherwise, it takes 0.

B. MODEL CONSTRUCTION

Suppose the total number of stations in the network is L. S_t, I_t, and R_t are respectively the number of stations prone to

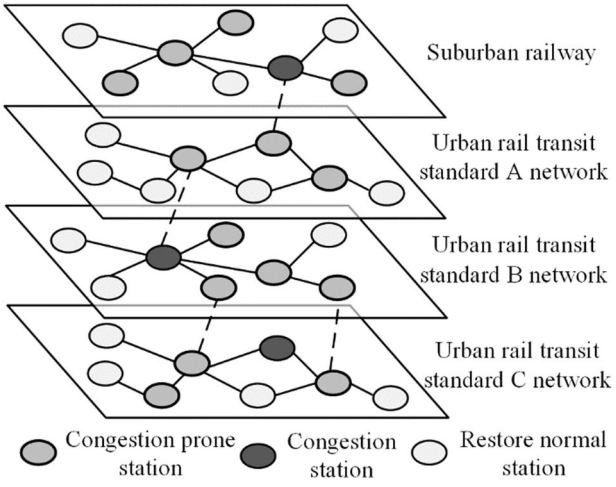

FIGURE 6. Multi-level rail transit network congestion propagation process.

congestion, congestion, and congestion relief in the network at time t. A station in a congested state affects adjacent stations, which are prone to congestion at a propagation rate λ. At the same time, the congested station gradually returns to normal status at a recovery rate μ. Fig. 6 shows the multi-level rail transit network congestion propagation process.

Based on the SIR model, the relationship between the three types of stations is

$$\begin{cases} \Delta S_{t+1} = -\lambda_t S_t I_t \\ \Delta I_{t+1} = \lambda_t S_t I_t - \mu_t I_t \\ \Delta R_{t+1} = \mu_t I_t \\ S_t + I_t + R_t = L \end{cases} \tag{21}$$

Assuming that the node degree of the congested station is N, the number of newly added congested stations in the network at time t is the difference between the number of congested stations propagated at that time and the number of restored regular stations, expressed as expectation:

$$\mathrm{E}(-S) = N\lambda_t - \mu_t I_t \tag{22}$$

Then, the network congestion propagation model at time t is

$$\begin{cases} \Delta I_{t+1} = (N\lambda_t - \mu_t I_t) I_t - \mu_t I_t \\ I_{t+1} = I_t + \Delta I_{t+1} \end{cases} \tag{23}$$

The tidal phenomenon of passenger flow leads to the imbalance of passenger flow in the direction of train operation. Fig. 7 shows the directional imbalance diagram in cross-station mode.

To quantify the imbalance of passenger flow distribution on the line, "main passenger flow direction node degree" N^1, N^2, N^3 are introduced. Among them, N^1 represents the number of adjacent stations of the congested station in the main passenger flow direction of the line. N^2 represents the number of adjacent stations of the congested station in the main passenger flow direction of the transfer line. N^3 represents the number of adjacent stations of the congested station in the main passenger flow direction of other rail transit lines.

The "directional imbalance coefficient" is used to reflect the degree of imbalance of passenger flow. The calculation method is as follows:

$$\kappa = \frac{2 \times \mathrm{Max}\{Q_{\mathrm{up}}, Q_{\mathrm{down}}\}}{Q_{\mathrm{up}} + Q_{\mathrm{down}}} \tag{24}$$

where Q_{up} is the maximum passenger flow in the upward section. Q_{down} is the maximum passenger flow in the downward section.

When $\kappa > 1.2$, the directional imbalance of passenger flow during peak periods is particularly prominent. Currently, congestion mainly propagates to stations in the main passenger flow direction. The values of N^1, N^2, and N^3 depend on the node degree in the main passenger flow direction. On the contrary, if $\kappa \leq 1.2$, it means that the passenger flow distribution of the line in the upward and downward directions is relatively balanced, and the congestion phenomenon propagates to both directions simultaneously. Currently, the values of N^1, N^2, and N^3 should be the sum of the node degrees in the up and down directions. In a multi-level rail transit network, the total number of nodes that congestion stations may propagate to is

$$N = N^1 + \sum_{w=1}^{W} N_w^2 + \sum_{d=1}^{D-1} N_d^3 \tag{25}$$

Considering factors such as train operation direction, station type, and passenger travel choice behavior in the process of congestion propagation, the number of new congested stations in the network at time t is

$$\begin{aligned} \mathrm{E}(-S) = \sum_{e=1}^{I} (N_e^1 \lambda_{te}^1 + \tau_e \sum_{w=1}^{W_e} N_{ew}^2 \lambda_{tew}^2 \\ + \varpi_e \sum_{d=1}^{D_e-1} N_{ed}^3 p_{hm}(d) \lambda_{ted}^3) - \mu_t I_t \end{aligned} \tag{26}$$

where I is the number of congested stations. W_e is the total number of transfer lines of congested station e. λ_{te}^1 is the propagation rate of congested station e on this line at time t. λ_{tew}^2 is the propagation rate of congested station e on transfer line w at time t. λ_{ted}^3 is the propagation rate of congested station e in the line of adjacent rail transit d at time t. N_e^1 is the node degree of the congested station e in the main passenger flow direction of this line. N_{ew}^2 is the node degree of congested station e in the main passenger flow direction of transfer line w. N_{ed}^3 is the node degree of the congested station e in the main passenger flow direction of the line of adjacent rail transit d. τ_e is a 0-1 variable. If the congestion station e is a transfer station within a certain mode of rail transit, it takes 1; otherwise, it takes 0. $p_{hm}(d)$ is the proportion of passengers transferring from sub-network o to sub-network d, which is represented by the probability of choosing travel mode d between h and m.

In summary, the multi-level rail transit passenger flow congestion propagation model considering passenger travel

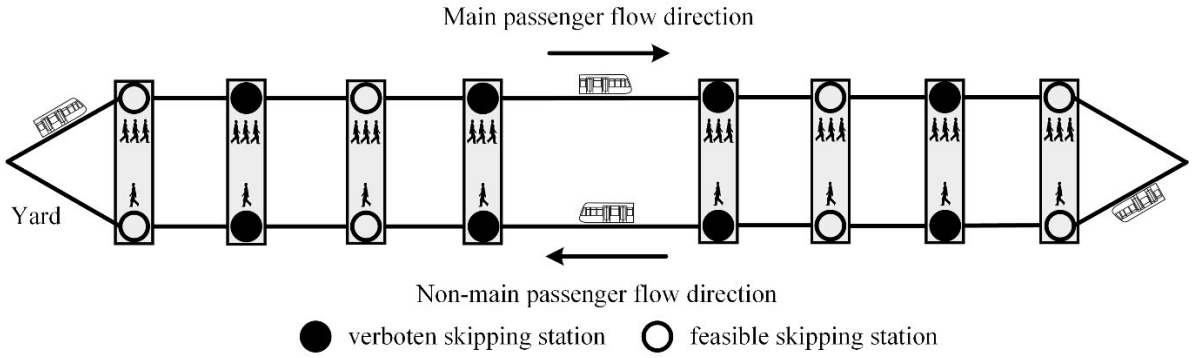

FIGURE 7. Directional imbalance diagram in cross-station mode.

choice behavior and train stopping schemes is

$$\begin{cases} \Delta I_{t+1} = [\sum_{e=1}^{I_t} (N_e^1 \lambda_{te}^1 + \tau_e \sum_{w=1}^{W_e} N_{ew}^2 \lambda_{tew}^2 \\ +\varpi_e \sum_{d=1}^{D-1} N_{ed}^3 p_{hm}(d) \lambda_{ted}^3) - \mu_t I_t] I_t - \mu_t I_t \\ I_{t+1} = I_t + \Delta I_{t+1} \end{cases} \tag{27}$$

The model fully considers the complexity of multi-level rail transit networks in its design, including the interconnections between different types of rail transit and the dynamic changes in passenger flow. By integrating multiple parameters, the model can accurately depict the congestion propagation mechanism of passengers under actual traffic conditions. Additionally, the infectious disease model operates quickly and can intuitively describe the law of congestion propagation, ensuring strong timeliness. This complexity and timeliness ensure that the model can adapt to diverse real-world scenarios, effectively capture the dynamic changes and cross-level propagation characteristics of passenger flow congestion, and provide precise prediction results.

IV. CASE ANALYSIS

Taking the multi-level rail transit network in Beijing, China as an example, the network includes subway, modern tram, suburban railway, maglev transit and other rail transit systems. During the red leaf viewing period of Xiangshan, since the terminal station of the XIJIAO Line is Fragrant Hills Station, the XIJIAO Line and its intersection line, Subway Line 10, are severely congested. Bagou Station is the interchange hub for the two lines. Analysis was conducted based on the passenger flow data of Beijing's multi-level rail transit on a certain day in October. Fig. 8 shows part of Beijing's multi-level rail transit network.

In 2023, Beijing residents' per capita disposable income $x = 81{,}800$ yuan/person, and the legal number of working days $q = 250$ days. According to the literature [39] and the actual situation, the penalty $B = 300$ yuan and the time value $T = 40.62$ yuan/h when the individual is late in the rigid travel. The average walking speed of passengers is $i = 1.29$ m/s. In the case of gain, the parameters of the weight function are $\delta = 0.72$, $\rho = 1.19$; in the case of loss, $\delta = 0.76$, $\rho = 1.21$. Based on the importance of travel time, cost, walking distance, and congestion degree, this study plans to set the cost conversion weight $\xi = 1$, the walking distance conversion weight $\upsilon = 1$, the decision preference coefficient of generalized travel time $\vartheta_u^k = 0.7$, and the decision preference coefficient of congestion degree $\vartheta_c^k = 0.3$. Table 2 shows the various indicators of the alternative travel scheme from Bagou Station to Fragrant Hills Park.

Table 2 shows that after the congestion at Bagou Station, the proportion of passengers transferred from the subway sub-network to the modern tram sub-network is 72.18 %. The congestion propagation rates of the XIJIAO Line and the subway Line 10 passing through the Bagou Station at different periods and in different directions are quantified. Fig. 9 and Fig.10 show the results.

Fig. 9 illustrates that due to commuting demand, the congestion propagation rate of the XIJIAO Line is significantly higher in the upward direction during the morning peak and in the downward direction during the evening peak. During the red leaf viewing period at Xiangshan, tourists are evenly distributed throughout the day, resulting in generally higher congestion propagation rates at other times. The continuity and dispersion of tourism activities significantly affect line congestion propagation.

Fig. 10 depicts that the congestion propagation rate of each station on Line 10 fluctuates significantly in the morning and evening peaks. The downward direction of Line 10 in the morning peak period is the main passenger flow direction, the upward direction is the non-main passenger flow direction, and the opposite in the evening peak period. In the upward direction, the propagation rate of Bagou Station (transfer station) reached 0.58 at 8:00-9:00 in the morning peak. The propagation rate of Lianhua Qiao Station reached 0.77 at 18:00-19:00 in the evening peak. In the downward direction, the propagation rate of Xidiaoyutai Station reached 0.87 at 8:00-9:00 in the morning peak and 0.58 at 17:00-18:00 in the evening peak.

FIGURE 8. Part of Beijing's multi-level rail transit network.

TABLE 2. Indicators of the alternative travel scheme.

Travel mode	Travel route	Travel time /min	Cost/yuan	walking distance /m	Average full load rate	Perceived utility	Selection probability
Tram	XIJIAO Line	43	4	944	1.25	0.0240	72.18%
	XIJIAO Line - Bus No. 563	54	6	917	1.25	-0.1223	
Subway + Bus	Line 10 - Line 16 - Bus No. 563	65	5	748	0.92	-0.2507	0.45%
	Line 10 - Line 4 - Bus No. 563	71	5	708	0.92	-0.6789	
Bus	Bus No. 630 - Bus No. 563	62	4	800	0.70	-0.1089	27.37%
	Bus No. 563	68	3	1300	0.70	-0.2700	

The congestion propagation range of the subway Bagou Station at different times of the day and recovery rates are analyzed. Fig. 11 shows the results.

Fig. 11 demonstrates that congestion spreads widely during morning and evening peak periods. As the recovery rate increases, the congestion propagation range decreases significantly. When $\mu = 0.1$, in the upward direction, the maximum congestion propagation range of Bagou Station at 8:00-9:00 in the morning peak is 12 stations, and the maximum congestion propagation range at 18:00-19:00 in the evening peak is 15 stations. In the downward direction, the maximum congestion propagation range at 8:00-10:00 in the morning peak is 14 stations, and the maximum congestion propagation range at 18:00-20:00 in the evening peak is 13 stations. Fig. 12 shows the data distribution of the congestion propagation range in Bagou Station.

Fig. 12 demonstrates that when $\mu = 0.1$, the dispersion of the number of congested stations is the largest. Currently, the number of congested stations in the upward direction is concentrated in the interval [9], [11], while the number of congested stations in the downward direction is concentrated in the interval [9], [12]. With the gradual recovery rate increase, the dispersion degree of the number of congested stations gradually decreases and finally concentrates in the interval [2], [3].

V. DISCUSSION AND ANALYSIS

A. PARAMETER ANALYSIS OF NL-PT MODEL

The NL-PT model's simulation experiment reveals the internal relationship between model parameters and various indicators. Fig. 13 and Fig. 14 show the results.

Fig. 13 demonstrates that there are apparent differences in the influence of the gain sensitivity coefficient and loss sensitivity coefficient on the prospect value of generalized travel time and congestion degree. Under the condition that the gain sensitivity coefficient remains unchanged, the prospect

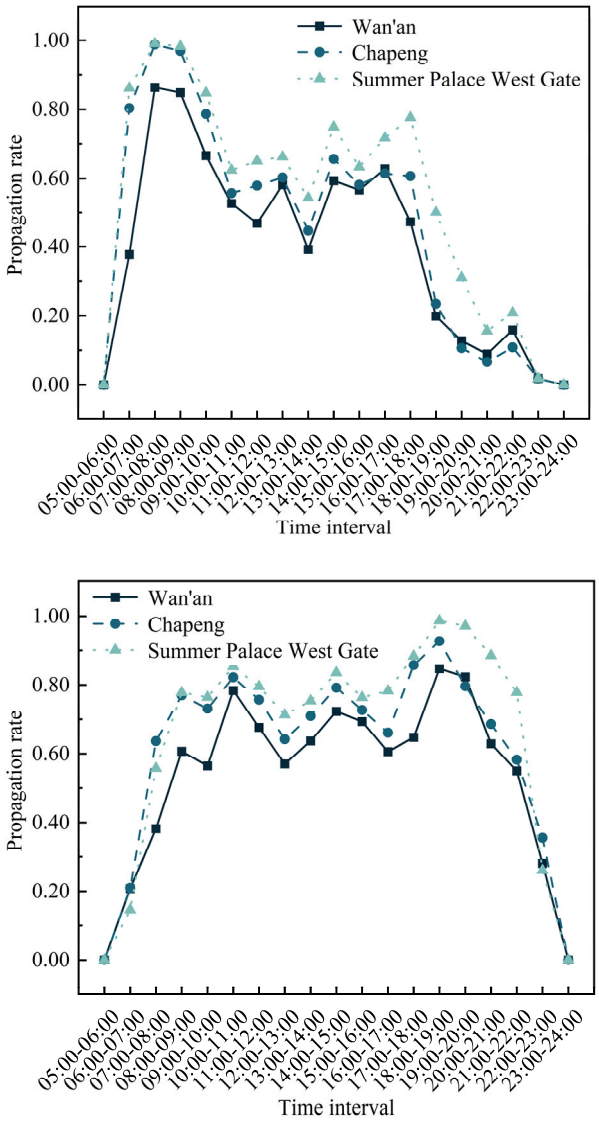

FIGURE 9. Congestion propagation rate of some stations on the XIJIAO Line. (a) Upward direction. (b) Downward direction.

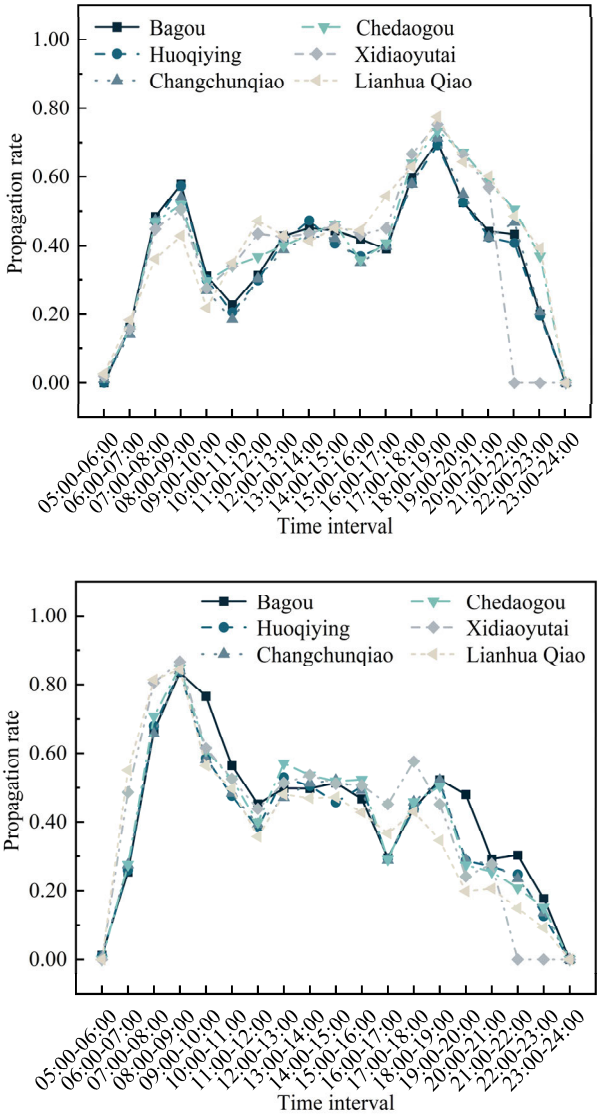

FIGURE 10. Congestion propagation rate of some stations on Line 10. (a) Upward direction. (b) Downward direction.

value of generalized travel time does not change with the change of loss sensitivity coefficient. However, the prospect value of the congestion degree shows a significant upward trend with the increase of the loss sensitivity coefficient. When the loss sensitivity coefficient is constant, the travel time prospect value will gradually increase with the increase of the gain sensitivity coefficient. The gain sensitivity coefficient does not affect the prospect value of congestion degree, showing its relative stability to the gain change.

Fig. 14 shows that the attraction parameter ρ and discrimination parameter δ influence passengers' travel path prospect value and mode selection probability differently. When δ is constant, increasing ρ decreases travel time prospect value but increases congestion prospect value, overall prospect value, and mode selection probability. This indicates that ρ reflects passengers' preference for travel paths; higher ρ enhances comfort and service quality, reducing time sensitivity and increasing congestion tolerance, thus improving the likelihood of choosing that mode.

When ρ is constant, increasing δ raises the travel time prospect value and lowers the congestion prospect value, but the overall prospect value and selection probability remain nearly unchanged. This shows that while δ affects perceptions of time and congestion, it doesn't significantly impact the overall travel mode choice.

B. PARAMETER ANALYSIS OF CONGESTION PROPAGATION MODEL

The intrinsic relationship between the model parameters and congestion propagation is revealed by conducting sensitivity analysis on each parameter in the model. Fig. 15 shows the results.

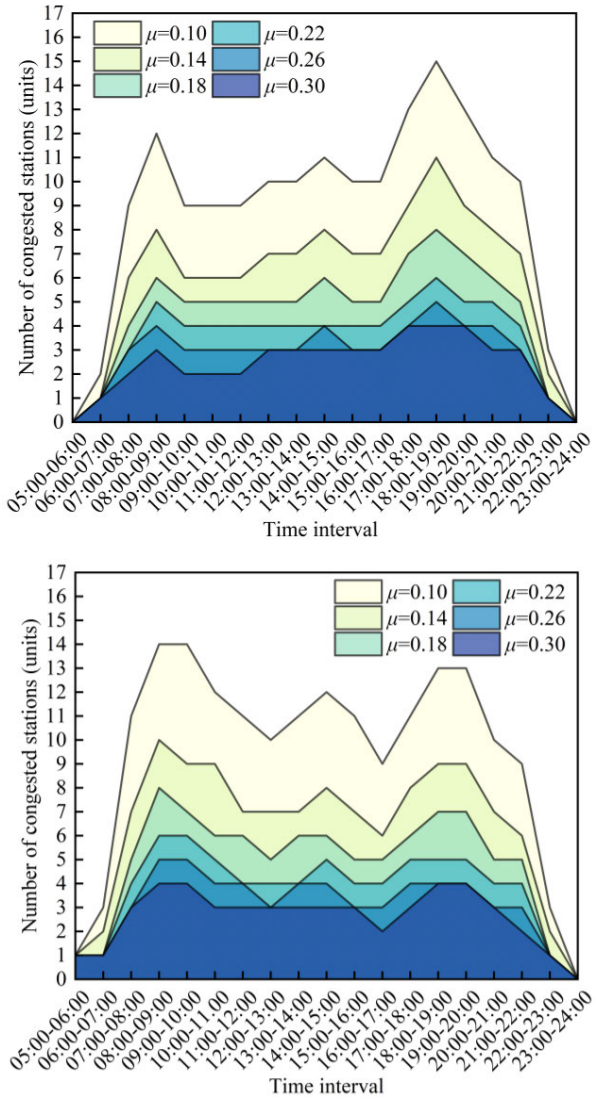

FIGURE 11. Congestion propagation range of Bagou Station. (a) Upward direction. (b) Downward direction.

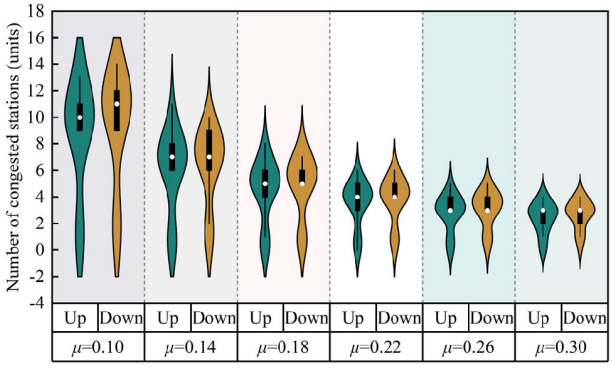

FIGURE 12. Data distribution of congestion propagation range in Bagou Station.

Fig. 15(a) demonstrates that when $\lambda \leq 0.2$, the initial congestion station gradually returns to normal; and when $\lambda > 0.2$, congestion will propagate to adjacent

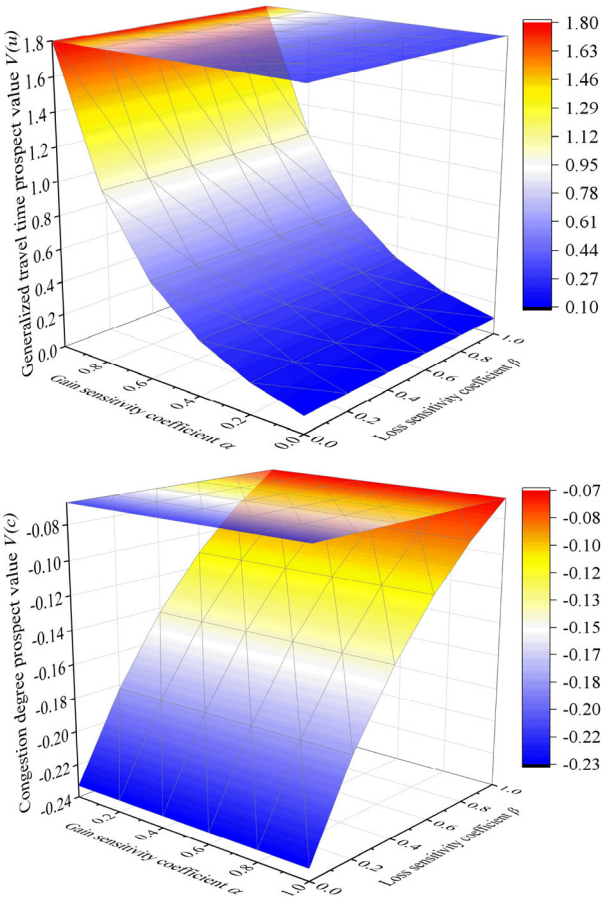

FIGURE 13. The impact of parameters α and β on various indicators. (a) The impact on generalized travel time prospects. (b) The impact on congestion deree prospects.

stations. The greater the propagation rate, the greater the congestion propagation range. When $\lambda = 0.40$, congestion propagation fluctuates less. Within 2 to 16 minutes, the congestion propagation range fluctuates between 4 to 5 stations. After 16 minutes, the congestion propagation range stabilizes at 5 stations. When $\lambda = 0.5$, within 2 to 43 minutes, the congestion propagation range fluctuates between 4 to 7 stations. After 43 minutes, the congestion propagation range gradually stabilizes at 6 stations. When $\lambda = 0.6$, passenger flow congestion propagation shows prominent fluctuation characteristics. The propagation effect cannot dissipate automatically but appears as a reciprocating phenomenon. The congestion propagation range expands three times when the propagation rate increases from 0.3 to 0.6. The congestion propagation process shows significant volatility characteristics. When the volatility is low, timely and appropriate control measures can effectively control the propagation effect of congestion and prevent its further spread.

Fig. 15(b) demonstrates that when $\mu > 0.5$, the congestion phenomenon will hardly propagate, and the congested station can gradually return to the normal state. However,

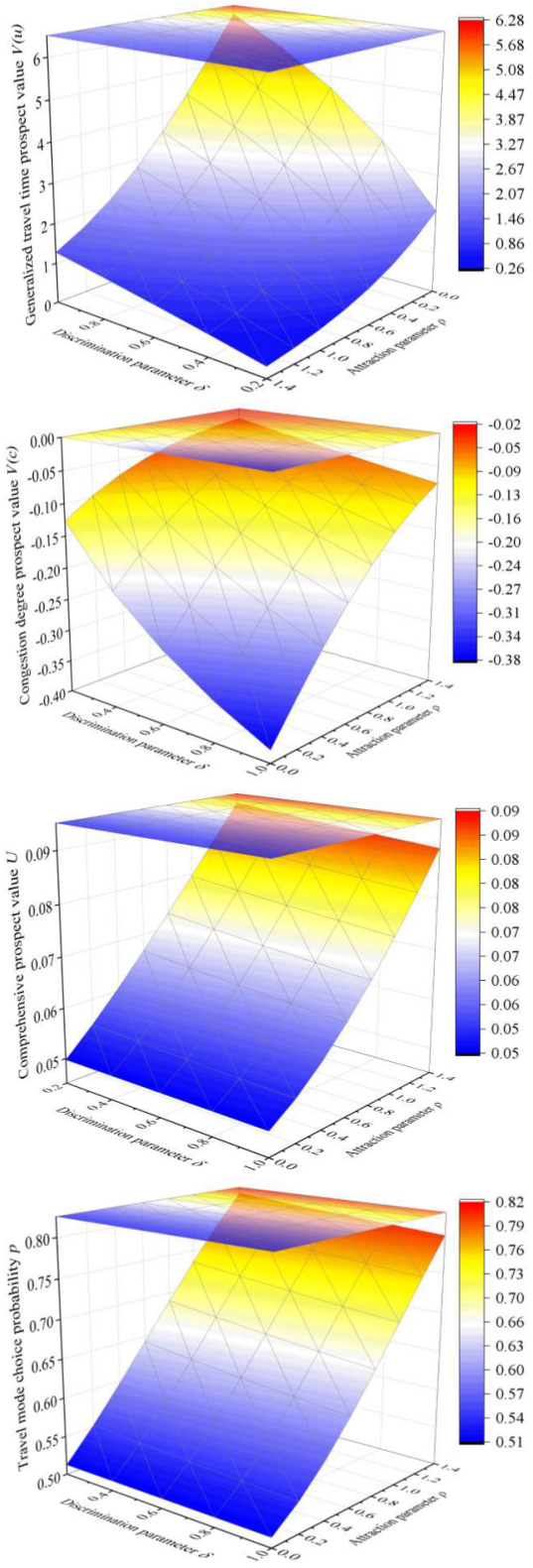

FIGURE 14. The impact of parameters δ and ρ on various indicators. (a) The impact on generalized travel time prospects. (b) The impact on congestion degree prospects. (c) The impact on the comprehensive prospect value. (d) The impact on travel mode choice probability.

when $\mu \leq 0.5$, congestion gradually propagates, and the size of the recovery rate has a significant impact on the congestion propagation range. The smaller the recovery rate, the more comprehensive the congestion propagation range, affecting up to 20 stations. When the recovery rate is reduced from 0.5 to 0.1, the congestion propagation range expands 6.8 times. When $\mu = 0.1$, congestion propagation appears volatile. Therefore, to effectively alleviate congestion propagation, it is crucial to take timely flow-limiting measures to improve the recovery rate.

Fig. 15(c) demonstrates that with the opening of the new rail transit system, people's travel demand has been further stimulated, and induced passenger flow has also occurred. This phenomenon directly leads to expanding the spread of congestion, putting more significant pressure on the already congested rail transit network. In particular, when $D \geq 4$, congestion propagation shows apparent volatility, and as the number of rail transit network layers increases, the volatility gradually increases.

Fig. 15(d) demonstrates that a significant positive correlation exists between the number of passengers stranded on the platform and the extent of congestion. The greater the number of stranded passengers, the more comprehensive the congestion range, and the shorter the time it takes for the number of congested stations to reach its peak. In addition, the increase in the number of passengers stranded on the platform will also increase the volatility of congestion propagation, further exacerbating the network's instability.

Fig. 15(e) demonstrates that when congestion occurs at the station, the impact of the transfer ratio on adjacent rail transit systems is significantly different. Specifically, the greater the transfer ratio, the more prominent its effects on adjoining rail transit lines, further aggravating the spread of congestion. When $p \geq 0.6$, congestion propagation volatility increases significantly, network stability will be seriously affected, showing high instability.

Fig. 15(f) demonstrates that as the proportion of waiting passengers heading to subsequent stops of the arriving train increases, the congestion propagation rate and congestion propagation range also increase accordingly. This shows that the more train stops, the more likely congestion will occur and spread more quickly. When $\varphi \geq 0.6$, slight fluctuations will occur in the early stages of congestion propagation. However, after a few minutes of development, the congestion propagation range stabilizes at a fixed value. When the ratio is 1, congestion can spread to a maximum of 5 stations; when the ratio is 0, congestion can spread to a maximum of 4 stations, which is 20% less than when the ratio is 1. If this proportion decreases by 80%, the congestion propagation range decreases by 23.3%.

Fig. 15(g) demonstrates that the congestion propagation range is not directly affected by the number of initial congested stations but will gradually converge to a stable state. Additionally, as the number of initial congested stations increases gradually, the time required to reach the maximum propagation range will decrease accordingly.

Fig. 15(h) demonstrates that when congestion occurs at terminal and intermediate stations, the impact range is relatively

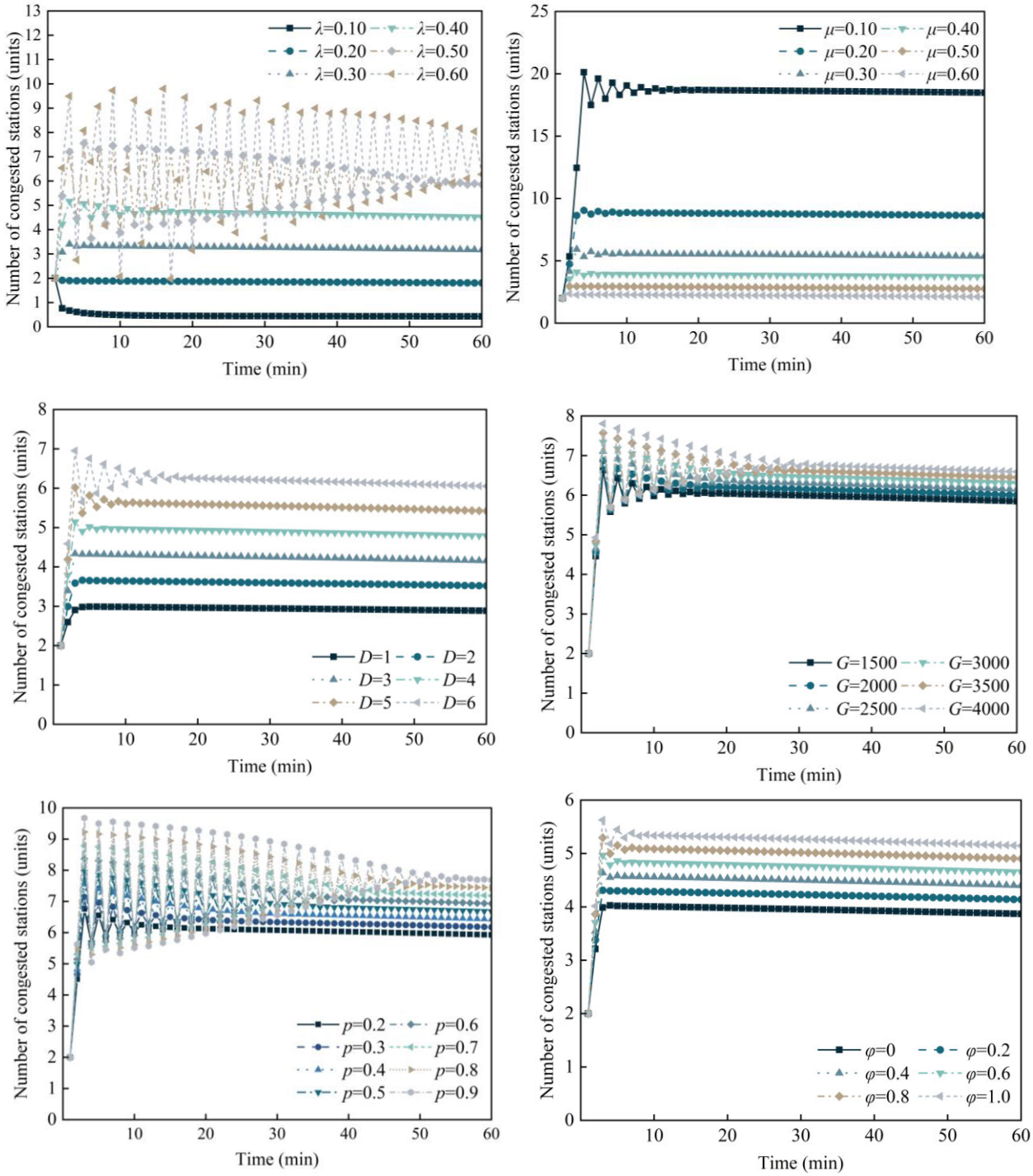

FIGURE 15. The impact of SIR model parameters on the congestion propagation range. (a) Propagation rate λ. (b) Recovery rate μ. (c) Number of network layers D. (d) Number of passengers stranded on the platform G. (e) Transfer ratio p. (f) Proportion of waiting passengers heading to subsequent stops of the arriving train φ. (g) The number of initial congested stations I_0. (h) Node degree N.

limited. Congested stations can gradually return to normal, and the propagation effect at intermediate stations is slightly stronger than at terminals. However, there is mutual interference among transfer passenger flows at transfer stations. Without effective diversion measures for transfer passenger flows, it is easy to cause intersections and mutual impacts. As a result, the degree of congestion propagation at transfer stations far exceeds that at terminal and intermediate stations. Additionally, the wider the network connectivity of a transfer station, the broader its congestion propagation range. When $N \leq 4$, there is almost no volatility in the congestion propagation range. After reaching the extreme value of the

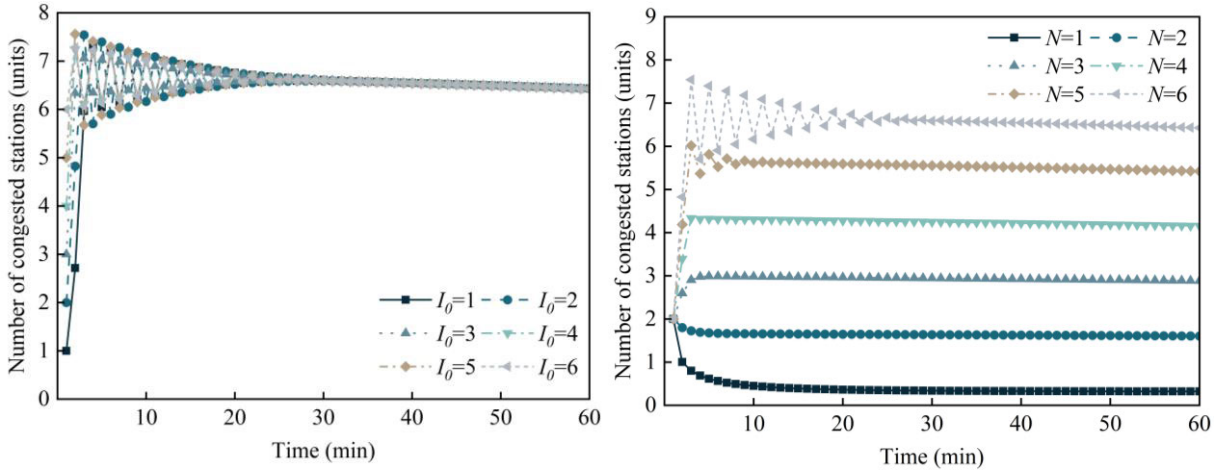

FIGURE 15. *(Continued.)* **The impact of SIR model parameters on the congestion propagation range. (a) Propagation rate λ. (b) Recovery rate μ. (c) Number of network layers *D*. (d) Number of passengers stranded on the platform *G*. (e) Transfer ratio *p*. (f) Proportion of waiting passengers heading to subsequent stops of the arriving train φ. (g) The number of initial congested stations I_0. (h) Node degree *N*.**

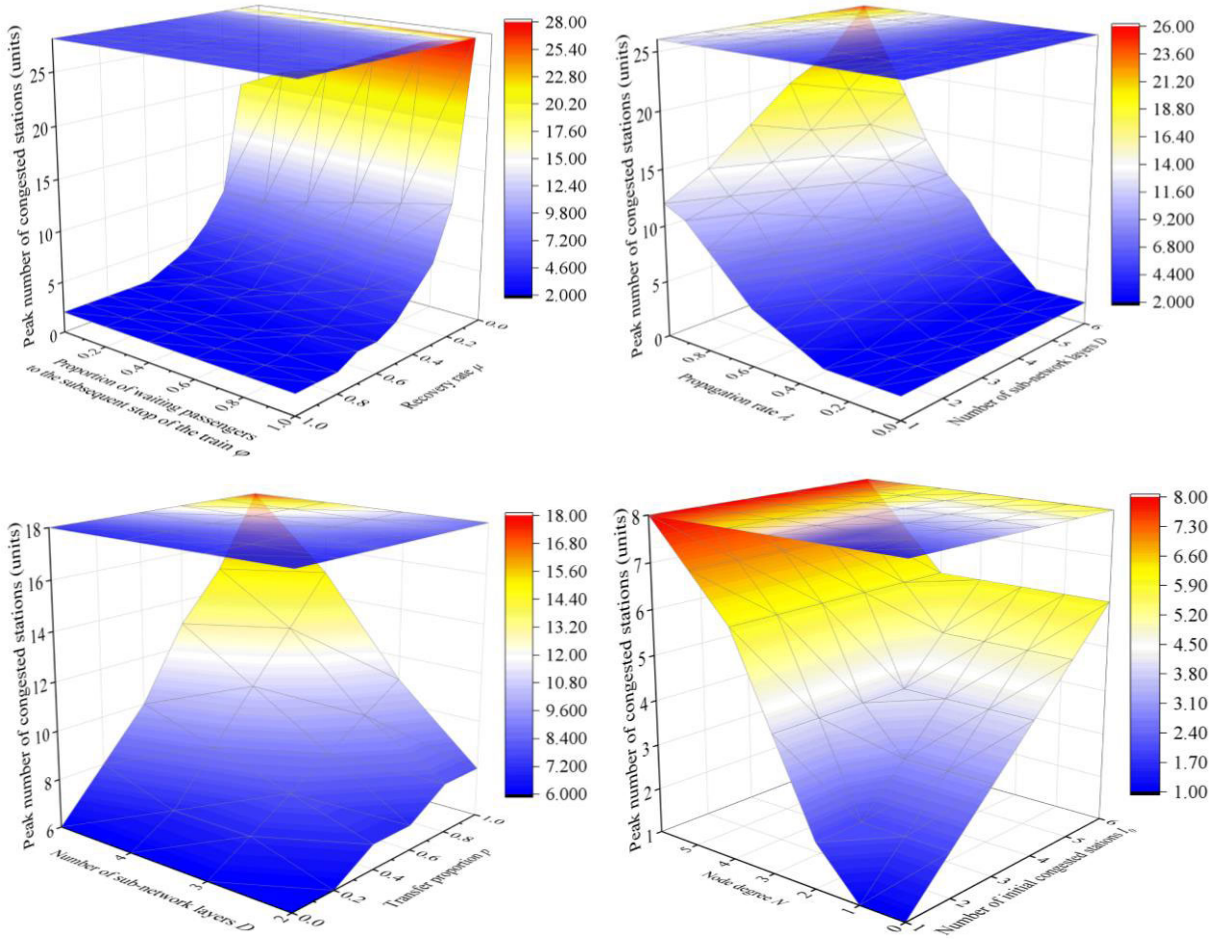

FIGURE 16. **The synergistic influence of SIR model parameters on the congestion propagation range. (a) Parameters φ and μ. (b) Parameters λ and *D*. (c) Parameters *D* and *p*. (d) Parameters *N* and I_0.**

congestion propagation range, it stabilizes at a constant value. When $N = 5$, there is slight volatility in the congestion propagation range, fluctuating between 4 to 6 stations within 2 to 8 minutes. When $N = 6$, there is significant volatility in

the congestion propagation range, fluctuating between 6 to 7 stations within 2 to 20 minutes.

The changing trend of congestion propagation range under different parameter combinations reveals the influence degree of the interaction between parameters on congestion propagation. Fig. 16 shows the results.

Fig. 16(a) depicts that the impact of the recovery rate μ on the congestion propagation range is significantly more significant than the proportion of waiting passengers heading to subsequent stops of the arriving train φ. Specifically, when φ remains unchanged, as μ increases, the congestion propagation range will decrease significantly. When μ maintains a certain level, as φ increases, the congestion propagation range will show an increasing trend, but it will be relatively small.

Fig. 16(b) depicts that when the propagation rate λ is small, the impact of the network layer D on the congestion propagation range is small. When $\lambda > 0.4$, the effect of D on the congestion propagation range is more significant. As D increases, the impact of λ on the congestion propagation range increases. Specifically, when λ is constant, the more D, the greater the congestion propagation range. When D is constant, the larger λ is, the more extensive the congestion propagation range will be.

Fig. 16(c) depicts that as the number of network layers D and the transfer ratio p increase, the congestion range shows an expanding trend. When $D \geq 3$, p has a more significant impact on the congestion propagation range. However, when $p < 0.4$, even if D increases, the congestion propagation range will not increase significantly.

Fig. 16(d) depicts that when the node degree $N \leq 1$, the congestion phenomenon will hardly propagate. The number of congested stations in the network is consistent with the number of initial congested stations I_0. This shows that the ability of congestion to spread is limited when nodes are less connected. However, when $N \geq 2$, the congestion propagation range is no longer restricted by I_0, and the total number of congested stations in the network will increase significantly. It shows that as the number of node connections increases, the propagation ability of congestion in the network increases. When I_0 remains unchanged, as N increases, the congestion propagation range will also expand accordingly.

VI. CONCLUSION

To effectively deal with the congestion propagation phenomenon that occurs in multi-level rail transit systems during periods of heavy passenger flow, the ''bounded rationality'' characteristics of passengers' travel decision-making are considered, and an NL-PT model that considers passengers' travel choice behavior is constructed based on prospect theory. A multi-level rail transit passenger flow congestion propagation model is further established by comprehensively considering factors such as the train stopping scheme and train running directions. The model is widely applicable to rail transit networks in most cities in China. When applied to other cities and countries, however, due to differences in transportation systems and urban planning, the model parameters still need to be appropriately adjusted and improved according to actual conditions. This ensures that the model can better adapt to the characteristics of passenger congestion propagation under different environments and conditions. The main conclusions are summarized as follows:

1) The more sensitive passengers are to the gains during travel, the more positive their expectations and perceptions of travel time will be. When the attraction parameter increases, passengers' prospect value and likelihood of choosing this travel mode will significantly increase. Compared to the attraction parameter, the enhancement of the discrimination parameter will affect passengers' perception of travel time and congestion level to a certain extent, but this effect is not significant.

2) Factors such as the propagation rate, recovery rate, number of network layers, number of passengers stranded on the platform, and transfer ratio have a significant impact on congestion propagation. When the congestion propagation rate is greater than 0.4, the number of layers of the multi-layer rail transit network has a particularly significant impact on the congestion propagation range. The more layers there are in the network, the more influential the bounded rationality characteristics of passengers' travel decisions affect congestion propagation.

3) As the node degree increases, the propagation paths of congestion in the network become richer, allowing congestion to spread to the entire network faster. When the node degree of a congested station is less than or equal to 1, its congestion diffusion ability is limited. When the node degree is greater than or equal to 2, the total number of congested stations in the network increases significantly. When the node degree is greater than or equal to 4, the congestion propagation range does not expand with the increase in the number of initially congested stations. Instead, it stabilizes at the maximum propagation range, increasing by 1 station for each increment in node degree.

4) A significant positive correlation exists between the number of train stops and the congestion propagation rate and scope. In addition, the more significant the proportion of waiting passengers heading to subsequent stops of the arriving train, the more widespread the congestion phenomenon will be among train stops. When the proportion of waiting passengers heading to the subsequent stops of the arriving train is greater than or equal to 0.6, slight fluctuations occur in the initial stage of congestion propagation. When the ratio is 1, congestion can spread to up to 5 stations; when the ratio is 0, congestion can spread to up to 4 stations, which is 20% less than when the ratio is 1. When this proportion decreases by 80%, the congestion propagation range decreases by 23.3%.

Through this model, the operating company can more accurately predict the trend and scope of passenger congestion in the multi-level rail transit network and promptly grasp the congestion levels within the network. This will help the company formulate and implement corresponding relief measures, such as adjusting train schedules, optimizing transfer schemes, and diverting passenger flow, to

effectively alleviate congestion. Additionally, the real-time data and predictive information provided by the model can assist decision-makers in optimizing the overall operational efficiency and service level of the transportation network, thereby improving the passenger travel experience.

REFERENCES

[1] C. Wright and P. Roberg, "The conceptual structure of traffic jams," *Transp. Policy*, vol. 5, no. 1, pp. 23–35, Jan. 1998, doi: 10.1016/s0967-070x(98)00006-7.

[2] J. Wu, Z. Gao, and H. Sun, "Simulation of traffic congestion with SIR model," *Modern Phys. Lett. B*, vol. 18, no. 30, pp. 1537–1542, Dec. 2004, doi: 10.1142/s0217984904008031.

[3] J. Zheng, Z. Zhu, H. Du, and Z. Gao, "Congestion and efficiency in complex traffic networks," *Int. J. Modern Phys. C*, vol. 24, no. 10, Oct. 2013, Art. no. 1350072, doi: 10.1142/s012918311350071x.

[4] S. Li, J. Wu, Z. Gao, Y. Lin, and B. Fu, "The analysis of traffic congestion and dynamic propagation properties based on complex network," *Acta Phys. Sinica*, vol. 60, no. 5, 2011, Art. no. 050701.

[5] M. Saberi, H. Hamedmoghadam, M. Ashfaq, S. A. Hosseini, Z. Gu, S. Shafiei, D. J. Nair, V. Dixit, L. Gardner, S. T. Waller, and M. C. González, "A simple contagion process describes spreading of traffic jams in urban networks," *Nature Commun.*, vol. 11, no. 1, Apr. 2020, Art. no. 1616, doi: 10.1038/s41467-020-15353-2.

[6] B. Priambodo, A. Ahmad, and R. A. Kadir, "Predicting traffic flow propagation based on congestion at neighbouring roads using hidden Markov model," *IEEE Access*, vol. 9, pp. 85933–85946, 2021, doi: 10.1109/ACCESS.2021.3075911.

[7] C. Du, X. Li, R. Sun, P. Zhang, and G. Zhu, "Classification of urban rail stations based on passenger flow congestion propagation," *J. Beijing Jiaotong Univ.*, vol. 45, no. 1, pp. 39–46, Feb. 2021, doi: 10.11860/j.issn.1673-0291.20200085.

[8] W. Chen, Z. Li, C. Liu, and Y. Ju, "Research on the number of passengers on the platform of rail transit station considering congestion propagation," *J. Syst. Simul.*, vol. 34, no. 7, pp. 1582–1592, Jul. 2022, doi: 10.16182/j.issn1004731x.joss.21-0198.

[9] M. Li, Y. Wang, J. Jin, and L. Jia, "Network congestion evolution law of urban rail transit based on network passenger flow mode," *J. Southeast Univ. Natural Sci. Ed.*, vol. 47, no. 2, pp. 404–409, Mar. 2017, doi: 10.3969/j.issn.1001-0505.2017.02.033.

[10] X. Ding, Y. Zhao, Z. Liu, and H. Hu, "The modeling of urban rail transit emergency delay propagation scope under network operation mode," *Concurrency Comput., Pract. Exper.*, vol. 32, no. 23, Dec. 2020, Art. no. e5530, doi: 10.1002/cpe.5530.

[11] Q. Zhang, W. Xiao, and G. Pan, "A CA-based simulation model of urban railway large passenger flow congestion transmission," *J. Transp. Syst. Eng. Inf. Technol.*, vol. 17, no. 4, pp. 83–89, Aug. 2017, doi: 10.16097/j.cnki.1009-6744.2017.04.013.

[12] Y. Jiang, W. Liu, and Z. Yao, "Evolution mechanism of congestion and dissipation of sudden passenger flow in urban rail transit based on cellular automaton," *J. Transp. Syst. Eng. Inf. Technol.*, vol. 20, no. 5, pp. 121–127, Oct. 2020, doi: 10.16097/j.cnki.1009-6744.2020.05.018.

[13] L. Sun, Y. Huang, Y. Chen, and L. Yao, "Vulnerability assessment of urban rail transit based on multi-static weighted method in beijing, China," *Transp. Res. A, Policy Pract.*, vol. 108, pp. 12–24, Feb. 2018, doi: 10.1016/j.tra.2017.12.008.

[14] A. Huang, H. M. Zhang, W. Guan, Y. Yang, and G. Zong, "Cascading failures in weighted complex networks of transit systems based on coupled map lattices," *Math. Problems Eng.*, vol. 2015, pp. 1–16, May 2015, doi: 10.1155/2015/940795.

[15] J. Zhang, Z. Wang, S. Wang, W. Shao, X. Zhao, and W. Liu, "Vulnerability assessments of weighted urban rail transit networks with integrated coupled map lattices," *Rel. Eng. Syst. Saf.*, vol. 214, Oct. 2021, Art. no. 107707, doi: 10.1016/j.ress.2021.107707.

[16] Z. Xiong and Z. Yao, "Influence scope of cascading failure on rail transit system," *J. Transp. Syst. Eng. Inf. Technol.*, vol. 20, no. 1, pp. 12–18, Feb. 2020, doi: 10.16097/j.cnki.1009-6744.2020.01.003.

[17] J. Zhang, S. Wang, and X. Wang, "Comparison analysis on vulnerability of metro networks based on complex network," *Phys. A, Stat. Mech. Appl.*, vol. 496, pp. 72–78, Apr. 2018, doi: 10.1016/j.physa.2017.12.094.

[18] B. Liu, G. Zhu, X. Li, and R. Sun, "Vulnerability assessment of the urban rail transit network based on travel behavior analysis," *IEEE Access*, vol. 9, pp. 1407–1419, 2021, doi: 10.1109/ACCESS.2020.3047159.

[19] Z. Xiong and Z. Yao, "Congestion propagation quantization model about rail transit system," *J. Transp. Syst. Eng. Inf. Technol.*, vol. 18, no. 3, pp. 146–151, Jun. 2018, doi: 10.16097/j.cnki.1009-6744.2018.03.023.

[20] Z. Zeng and T. Li, "Analyzing congestion propagation on urban rail transit oversaturated conditions: A framework based on SIR epidemic model," *Urban Rail Transit*, vol. 4, no. 3, pp. 130–140, Aug. 2018, doi: 10.1007/s40864-018-0084-6.

[21] Z. Shi, N. Zhang, and L. Zhu, "Understanding the propagation and control strategies of congestion in urban rail transit based on epidemiological dynamics model," *Information*, vol. 10, no. 8, p. 258, Aug. 2019, doi: 10.3390/info10080258.

[22] X. Wang, E. Yao, and S. Liu, "Simulation of metro congestion propagation based on route choice behaviors under emergency-caused delays," *Appl. Sci.*, vol. 9, no. 20, p. 4210, Oct. 2019, doi: 10.3390/app9204210.

[23] R. Ding, J. Yin, P. Dai, L. Jiao, R. Li, T. Li, and J. Wu, "Optimal topology of multilayer urban traffic networks," *Complexity*, vol. 2019, pp. 1–19, Oct. 2019, doi: 10.1155/2019/4230981.

[24] J. Ma, M. Li, and H.-J. Li, "Traffic dynamics on multilayer networks with different speeds," *IEEE Trans. Circuits Syst. II, Exp. Briefs*, vol. 69, no. 3, pp. 1697–1701, Mar. 2022, doi: 10.1109/TCSII.2021.3102577.

[25] Y. Zhang, Y. Li, M. Li, J. Ma, and Z. Qi, "An efficient resource allocation strategy for multilayer networks," *Int. J. Modern Phys. B*, vol. 35, no. 5, Feb. 2021, Art. no. 2150073, doi: 10.1142/s0217979221500739.

[26] L. Gao, P. Shu, M. Tang, W. Wang, and H. Gao, "Effective traffic-flow assignment strategy on multilayer networks," *Phys. Rev. E, Stat. Phys. Plasmas Fluids Relat. Interdiscip. Top.*, vol. 100, no. 1, Jul. 2019, Art. no. 012310, doi: 10.1103/physreve.100.012310.

[27] Y. Zhou, Y. Li, R. Jiang, and E. Geng, "Dynamic analysis of interactive transmission of warning information and traffic congestion," *J. Geo-Inf. Sci.*, vol. 19, no. 10, pp. 1279–1286, Oct. 2017.

[28] J. H. Huang, M. G. Sun, and Q. Cheng, "Congestion risk propagation model based on multi-layer time-varying network," *Int. J. Simul. Model.*, vol. 20, no. 4, pp. 730–741, Dec. 2021, doi: 10.2507/ijsimm20-4-585.

[29] H. Guo and L. Xu, "Research on the application of big data visualization technology in urban road congestion," *Eur. J. Remote Sens.*, vol. 56, no. 1, Dec. 2023, Art. no. 2147448, doi: 10.1080/22797254.2022.2147448.

[30] J. Huang and M. Sun, "Multi-network congestion risk propagation model considering driver behavior," *J. Transp. Syst. Eng. Inf. Technol.*, vol. 21, no. 1, pp. 8–15, Feb. 2021, doi: 10.16097/j.cnki.1009-6744.2021.01.002.

[31] C. Zhu, X. Ma, X. Wang, J. Fang, J. Wang, and L. Cheng, "Congestion propagation of double-layer urban rail transit considering passengers' bounded rationality," *IAENG Int. J. Appl. Math.*, vol. 53, no. 4, pp. 1230–1243, Dec. 2023.

[32] J. Jia, C. Zhu, J. Fang, J. Wang, L. Cheng, and C. An, "Research on congestion propagation of multi-level rail transit passenger flow based on SIR," *J. Lanzhou Jiaotong Univ.*, vol. 42, no. 3, pp. 39–45, Jun. 2023, doi: 10.3969/j.issn.1001-4373.2023.03.006.

[33] J. Zhou, W. Li, and Q. Luo, "Adjustment for train operation under the condition of mass passenger flow in urban rail transit," *J. Shenzhen Univ. Sci. Eng.*, vol. 37, no. 6, pp. 617–622, Nov. 2020, doi: 10.3724/sp.j.1249.2020.06617.

[34] F. Meng, L. Yang, Y. Lu, and R. Guo, "Collaborative optimization of urban rail transit operation and passenger flow control at stations using skip-stop pattern strategy," *J. Transp. Syst. Eng. Inf. Technol.*, vol. 21, no. 3, pp. 156–162, Jun. 2021, doi: 10.16097/j.cnki.1009-6744.2021.03.019.

[35] Z. Hu, Y. Xia, J. Cai, and F. Xue, "Optimization of urban rail transit operation adjustment based on multiple strategies under delay," *J. Jilin Univ.(Eng. Technol. Ed.)*, vol. 51, no. 5, pp. 1664–1672, Sep. 2021, doi: 10.13229/j.cnki.jdxbgxb20200467.

[36] L. Tao, J. Shi, J. Yang, and X. Yang, "A safety-oriented optimization model for train skip-stop strategy of oversaturated metro lines," *J. Transp. Inf. Saf.*, vol. 40, no. 3, pp. 51–59, 2022, doi: 10.3963/j.jssn.1674-4861.2022.03.006.

[37] H. Zhang, F. Dou, Y. Wei, J. Liu, and Y. Ning, "Peak hour stopping scheme optimization of suburban line considering train capacity constraints," *J. Transp. Syst. Eng. Inf. Technol.*, vol. 23, no. 5, pp. 247–257, Oct. 2023, doi: 10.16097/j.cnki.1009-6744.2023.05.026.

[38] Q. Wang, L. Deng, K. Liu, and G. Xu, "Optimization model of urban rail transit subsidies based on travel fare," *J. Railway Sci. Eng.*, vol. 21, no. 1, pp. 354–362, Jan. 2024, doi: 10.19713/j.cnki.43-1423/u.T20230213.

[39] Y. Huang, F. Yang, D. Zhang, and Y. Zeng, "Optimization of travel mode choice based on MA-CPT model," *J. Southwest Jiaotong Univ.*, vol. 58, no. 2, pp. 367–372, Apr. 2023.
[40] D. Kahneman and A. Tversky, "Prospect theory: An analysis of decision under risk," *Econometrica*, vol. 47, no. 2, p. 263, Mar. 1979.

CHANGFENG ZHU is currently a Professor and a Doctoral Tutor with the School of Traffic and Transportation, Lanzhou Jiaotong University, China. He was a National Railway Group Freight Safety Risk Management Expert and the Head of Excellent Scientific Research Team for Transportation System Optimization and Decision-Making. He has published more than 80 papers in authoritative journals and international conferences and presided over more than 60 scientific research projects, including the National Natural Science Foundation of China and major railroad systemic projects. His research interests include transportation system optimization and decision-making, transportation planning, and management.

JINXIU JIA received the B.S. degree in transportation from Lanzhou Jiaotong University, Lanzhou, China, in 2022, where she is currently pursuing the M.S. degree in transportation planning and management. Her main research interest includes multi-level rail transit operation organization.

JINHAO FANG received the M.S. degree in control engineering from Lanzhou Jiaotong University, Lanzhou, China, in 2020, where he is currently pursuing the Ph.D. degree in transportation planning and management. His main research interest includes complex networks.

JIE WANG received the M.S. degree in transportation planning and management from Beijing Jiaotong University, Beijing, China, in 2016. She is currently pursuing the Ph.D. degree in transportation planning and management with Lanzhou Jiaotong University, Lanzhou, China. Her main research interest includes rail transportation organization.

LINNA CHENG received the M.S. degree in transportation planning and management from Lanzhou Jiaotong University, Lanzhou, China, in 2014, where she is currently pursuing the Ph.D. degree in transportation planning and management. Her main research interest includes rail transportation organization.

RUNTIAN HE received the M.S. degree in engineering management from Lanzhou Jiaotong University, Lanzhou, China, in 2023, where he is currently pursuing the Ph.D. degree in transportation planning and management. His research interests include deep learning and intelligent transportation.

CHAO ZHANG received the M.S. degree in transportation planning and management from Lanzhou Jiaotong University, Lanzhou, China, in 2019, where he is currently pursuing the Ph.D. degree in transportation planning and management. His research interests include rail transportation organization optimization and railway traffic organization.